

# Application of a modified strain transient dip test in the determination of the internal stresses of PVC under tension

S. H. TEOH, C. L. CHUAH, A. N. POO

*Department of Mechanical and Production Engineering, National University of Singapore, Kent Ridge, Singapore 0511*

A modified strain transient dip test which involves the design of a load reduction apparatus to perform rapid step unloading and extrapolating to zero extension rate has been developed to measure the internal stresses (recovery and effective stress) of PVC under uniaxial tension. This simple technique appears to be consistent with other internal stress measurement techniques. It was found that the effective stress approaches a limiting value with applied strain and an extrapolated yield point could be defined. The limiting value is a function of the strain rate during the initial load application. The general increase in applied stress (at fixed applied strain) with crosshead speed was attributed to the increase in magnitude of the effective stress. The maximum peak ratio of effective over recovery stress, at each crosshead speed, could indicate that it was the energy-dissipating part of the material that played a dominant role in the early stages of the deformation while the energy-storage part dominated the latter stages.

## 1. Introduction

In order to investigate the deformation of materials, numerous authors [1-4] have partitioned the applied stress ( $\sigma_{ap}$ ) into internal stress components, namely effective stress ( $\sigma_{ef}$ ) and recovery stress ( $\sigma_{re}$ ). Mathematically this can be expressed as

$$\sigma_{ap} = \sigma_{ef} + \sigma_{re} \quad (1)$$

The recovery stress is responsible for restoring the deformed material into its original state, while the effective stress is responsible for bringing about the rate-activated deformation process of viscous flow [5].

The importance of such a partition of the applied stress is that it allows one to study in detail which stress component is responsible for, or plays a major role in, the ultimate failure of the material. However, measurement of these stress components is not easy as it depends on numerous factors such as applied load and strain, sensitivity of equipment and the type of model used to interpret the results [6].

In the continuing effort to study how  $\sigma_{ef}$  and  $\sigma_{re}$  are related to failure, the present work reports on the variation of these two stress components with deformation of polyvinyl chloride (PVC) under uniaxial tension. Special attention is given to the technique of measuring these internal stress components.

### 1.1. Measurement of internal stress components

Extensive work has already been carried out to determine the recovery and effective stresses in metals [3, 4, 7-9]. However, in the field of polymer science, this is less extensive. The recovery/effective stress measure-

ment techniques in polymers have been mainly derived from those developed for internal stress measurements of metals [1]. At present, there are three commonly used techniques in the measurement of the recovery/effective stress. These techniques are:

1. The strain transient dip test [9-12] which is mainly used for specimens subjected to constant load (creep) conditions.
2. The stress transient dip test [1, 2, 4, 13] which is mainly used for specimens subjected to a constant strain rate.
3. Stress relaxation methods [8, 14] which are mainly used for specimens subjected to constant strain conditions.

The latter two techniques have been adequately described by the many authors cited in the references above. Only the strain transient dip test, which is relevant to this paper, will be described in detail in the section below.

### 1.2. Strain transient dip test

The strain transient dip test is sometimes referred to as a stress reduction test [15, 16] or a stress dip test [17]. It has two main advantages over the other methods mentioned above. Firstly, only a simple loading creep apparatus is needed and secondly, the test can be done in a relatively short time. It has only been applied to metals and there does not seem to be any cited literature that employs this technique on polymers. As such, the discussion on the strain transient dip test will be based mainly on those experiments that have been applied to metals.

From the literature, there are two different methods of determining the internal stress of metals using the strain transient dip test. The reasons for the different techniques apparently lie in the different strain transient responses observed for each material and also in differences in the sensitivity of the equipment used [3, 9, 10, 15, 16, 18, 19]. The two methods are

- (a) the alternate creep-creep-recovery method, and
- (b) the incubation period method.

### 1.2.1. The alternate creep-creep-recovery method

Ahlquist and Nix [9] were among the earliest researchers to use this method. Basically, this method relies on the load reductions made during a creep experiment. The constant load applied to the specimen is interrupted by a small reduction load.

Immediately after a load reduction, a rapid contraction (elastic response) is observed and, depending upon the magnitude of the reduction, the immediate extension rate ( $de/dt$ ) can either be positive, negative or zero. The load that remains on the specimen, after a load reduction that produces the zero extension rate condition ( $L_r$  in Fig. 1), is then taken to be the recovery stress [20].

The creep indicated by a positive extension rate is thought of as being controlled by the effective stress. An understanding of the above responses to load reduction can be made by rewriting Equation 1 as

$$\sigma_{ef} = \sigma'_{ap} - \sigma_{re} \quad (2)$$

where  $\sigma'_{ap}$  = stress immediately after load reduction. If  $\sigma'_{ap} > \sigma_{re}$ , then from Equation 2

$$\sigma_{ef} > 0 \quad \text{and} \quad de/dt > 0 \quad (\text{creep}) \quad (3)$$

If  $\sigma'_{ap} < \sigma_{re}$ , then

$$\sigma_{ef} < 0 \quad \text{and} \quad de/dt < 0 \quad (\text{recovery}) \quad (4)$$

However, if  $\sigma'_{ap} = \sigma_{re}$ ,

$$\sigma_{ef} = 0 \quad \text{and} \quad de/dt = 0 \quad (5)$$

As written, Condition 5 enables the recovery stress to be measured. The load that produces this zero extension rate condition gives the recovery stress. From Equation 1, knowing  $\sigma_{ap}$  and  $\sigma_{re}$ ,  $\sigma_{ef}$  can then be determined.

Here, it has to be pointed out that Condition 5 depends on how one interprets the significance of the

zero extension rate. This can be visualized by expressing the total strain ( $\epsilon_T$ ) as the sum of the elastic ( $\epsilon_e$ ), anelastic ( $\epsilon_a$ ) and plastic ( $\epsilon_p$ ) strains, that is

$$\epsilon_T = \epsilon_e + \epsilon_a + \epsilon_p \quad (6)$$

Here  $\epsilon_e$  is defined as the instantaneous (less than 1 sec) strain that is completely recoverable on stress removal;  $\epsilon_a$  is defined as the non-instantaneous time-dependent recoverable strain on stress removal; and  $\epsilon_p$  is defined as the permanent strain that does not change significantly with time, after the deforming stress is removed.

Taking the differential with respect to time, Equation 6 becomes

$$\dot{\epsilon}_T = \dot{\epsilon}_e + \dot{\epsilon}_a + \dot{\epsilon}_p \quad (7)$$

The strain transient dip test requires that  $\dot{\epsilon}_T = 0$ . Equation 7 then becomes

$$\dot{\epsilon}_a + \dot{\epsilon}_p = 0 \quad (8)$$

( $\dot{\epsilon}_e$  is by definition negligible in a creep experiment).

There are two possible ways of interpreting Equation 8, that is

- (i) by equation  $\dot{\epsilon}_a = -\dot{\epsilon}_p$ , and
- (ii) by assuming that  $\dot{\epsilon}_a = \dot{\epsilon}_p = 0$ .

The first interpretation implies that one condition for a zero total strain rate could just be a balance between the anelastic and plastic strain rates. With such an interpretation it can be seen that the zero total extension rate condition will not allow one to determine the recovery stress accurately. In fact, if the plastic strain rate is positive during the strain transient dip test, then the anelastic strain rate has to be negative in order to give a zero total extension rate. This can happen if the stress immediately after load reduction is less than the recovery stress (see Condition 4). Under these conditions, the stress that gives a zero extension rate condition will always be lower than the actual recovery stress. If this model is used the recovery or effective stress can only be determined if there is some way of determining the plastic strain rate after the stress reduction. However, at present there is no known technique that can be used for this type of test.

The second interpretation is easier to visualize than the first. It can be understood if one considers a model where  $(\dot{\epsilon}_a + \dot{\epsilon}_p) = 0$ ; the effective stress has to be zero since  $\dot{\epsilon}_p = 0$ , and therefore the stress that produces the zero total extension rate condition actually determines the recovery stress.

### 1.2.2. The incubation period method

The experimental set-up for this method is the same as for the previous method with the exception that the initial load reduction is large but not large enough to produce recovery and subsequent load reductions are made after creep recommences. A number of authors have found that an incubation time ( $\Delta t$ ) always exists before creep recommences after a stress reduction [10, 15, 17, 19]. The incubation period increases with subsequent stress reductions ( $\Delta\sigma$ ). A plot of the sum of stress reduction ( $\Sigma\Delta\sigma$ ) against the sum of the incubation period ( $\Sigma\Delta t$ ) will show that  $\Sigma\Delta\sigma$  reaches a limiting value ( $\Sigma\Delta\sigma_{\text{limit}}$ ).

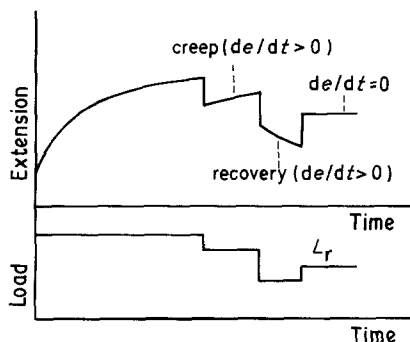


Figure 1 The alternate creep-creep-recovery method of measuring internal stresses of materials.

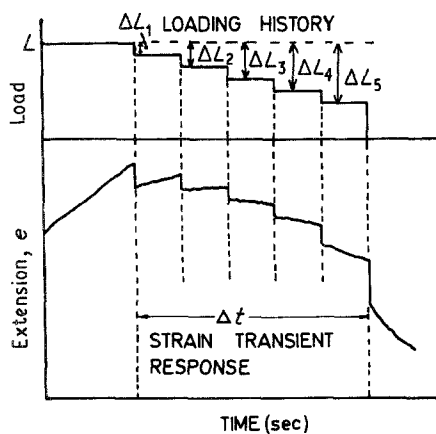


Figure 2 Schematic drawing of the modified strain transient dip test.

The recovery stress is then calculated by subtracting the limit  $\Sigma\Delta\sigma_{\text{limit}}$  from the applied stress, that is

$$\sigma_{\text{re}} = \sigma_{\text{ap}} - \Sigma\Delta\sigma_{\text{limit}} \quad (9)$$

and

$$\sigma_{\text{ef}} = \Sigma\Delta\sigma_{\text{limit}} \quad (10)$$

### 1.3. Strain transient dip test as applied to polymers

From Section 1.2, it can be seen that the question as to whether or not the strain transient dip test can be applied to polymers seems to depend upon how one interprets the strain transient dip tests with respect to the mathematical models and upon what type of strain transient responses are observed for the polymers.

Recent work on the transient response of high-density polyethylene showed that no incubation phenomenon was observed [2, 6]. As such, the incubation period method for the determination of the recovery stress in polymers may not be appropriate. The alternate creep-creep-recovery method seems suitable. However, in order to avoid errors due to relaxation of the test specimen during testing, some modification may be needed.

At this stage it is worth noting that the strain transient dip test need not be restricted to only constant-load creep experiments. With special design consider-

ations, it can be applied to tests in which the initial deformation is under a constant strain rate. The following section describes such a method.

## 2. Experimental procedure

### 2.1. Material and specimens

The PVC came in rigid glass-clear pressed sheets of thickness 1 mm and designated "Sunloid A-100" by the supplier (Tsutsunaka Plastic Industry, Japan). This material was widely used for transparent coverings of chemical equipment and components of appliances which require high clarity and good durability.

Test specimens conforming to ASTM D638, Type II were cut from the PVC sheet using a polymer router which had a cutting speed of 24 000 r.p.m. This high cutting speed was chosen because it gave a consistent and clean surface finish.

### 2.2. Modified strain transient dip test

The modified strain transient dip test involved small load reductions at regular intervals and simultaneous monitoring of the extension rate (see Fig. 2). Fig. 3 shows a schematic drawing of the strain transient dip test apparatus which was designed to be used on an Instron Universal Testing Machine under constant crosshead speed. The total extension rate was recorded by a linear variable displacement transducer (LVDT) (Schaevitz model 500 HR, Schaevitz Engineering, USA) placed parallel to the direction of uniaxial displacement. The signal from the transducer was conditioned via a signal conditioner and the output was recorded on a chart recorder.

The load reduction unit had a bottom plate which was bolted to the moving crosshead, thus ensuring negligible movement between the load reduction unit and the moving crosshead during straining of the specimen. Four to five load reductions using dead weights were used. Preliminary experiments had to be carried out first to determine the total weight of the reduction load that would be required for each test.

The strain transient dip test was carried out in such a way that when the applied load had reached a predetermined value, the crosshead was momentarily stopped. Stoppers A and B (Fig. 3) were then released

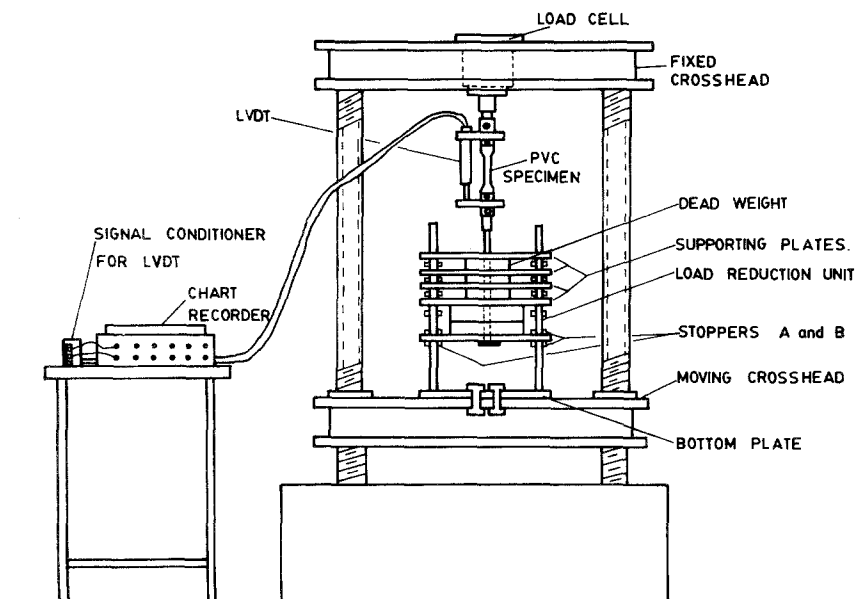


Figure 3 Schematic illustration of the modified strain transient dip test apparatus fitted on an Instron Universal Testing Machine.

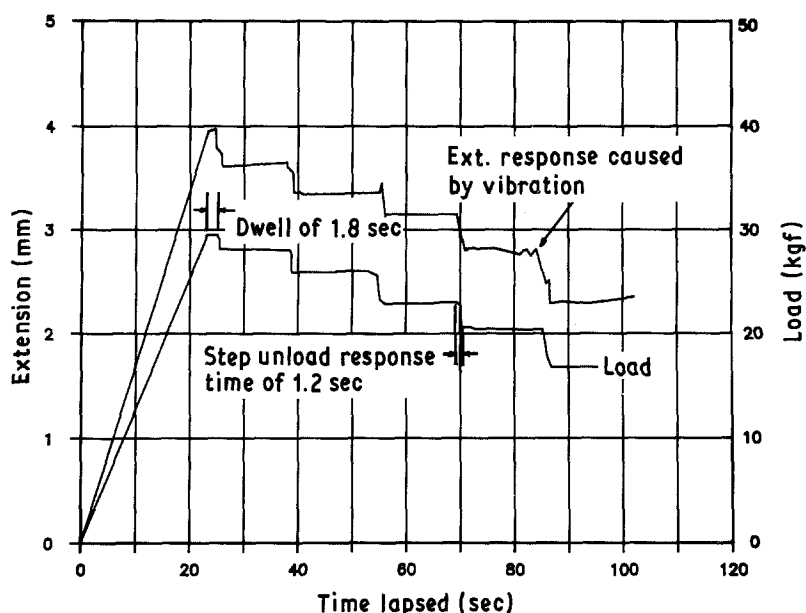


Figure 4 Typical results of the extension response to load reduction.

so that the weight acting on the specimen was reduced to those on the supporting plates. The crosshead was then moved in the reverse direction at the maximum crosshead speed of  $50 \text{ cm min}^{-1}$ , so that the weights acting on the specimens could be decreased incrementally. This was made possible by adjusting the stoppers below each supporting plate to increasing distance so that upon the reversal of the moving crosshead, the stoppers touched and lifted the first supporting plate, followed by the second, third and fourth.

Six crosshead speeds ranging from  $0.05$  to  $2.00 \text{ cm min}^{-1}$  were used. One specimen was used for each series of load reductions. This is because structural elements that give rise to the recovery stress may themselves relax [1]. In such a case, if more than one series of load reductions is performed on the same specimen, at different applied loads, the variation of recovery stress may not be representative for the particular crosshead speed. For each crosshead speed, the recovery stress for six applied stresses (mean values of 26.5, 31.7, 37.1, 44.0, 48.6 and 55.6 MPa) prior to yielding were determined. Three specimens were used for each applied stress. The tests were carried out at strains below the nominal yield strain (about 4% at  $0.05 \text{ cm min}^{-1}$  and 3.5% at  $2.00 \text{ cm min}^{-1}$ ) as the deformation below the nominal yield point is not complicated by necking and general yielding.

Typical results of the extension response to load reduction are shown in Fig. 4 for a crosshead speed of  $1.00 \text{ cm min}^{-1}$ . It can be noted that a small time delay of about 1.8 sec was recorded just below the first load reduction. This was due to the time taken to loosen the stoppers A and B (see Fig. 3). The corresponding creep was subsequently recorded in the plot of extension against time. However, this was deemed negligible compared to the total time scale of the experiment and was assumed not to affect the recovery stress measurements. Occasional vibration of the load reduction unit was also recorded and assumed to affect the results only marginally, within the experimental error of less than 10%. (In order to reduce vibration and increase sensitivity, a closed loop servohydraulic test rig is currently under construction for such a test.)

By plotting the load reduction against the extension rate (Fig. 5), the load at which zero extension rate ( $de/dt$ ) occurs was determined. The intercept at which  $de/dt$  is zero was taken to be the effective load. The effective stress was obtained from the ratio of the effective load and the original cross-sectional area of the specimen. The recovery stress was determined by subtracting the effective stress from the applied stress (ratio of the applied load and original area). Since the LVDT registers the total displacement between the grips on the specimen, the applied strain was obtained by dividing the total extension at the applied load by an effective gauge length of 104 mm. This effective gauge length was determined from a knowledge of the geometry of the specimen [21]. However, this method of determining the effective gauge length may not be the most accurate method, but as a first approximation, this is good enough for the present study.

All tests were performed at  $23 \pm 1^\circ \text{C}$  and  $65 \pm 5\%$  relative humidity.

### 3. Results and discussion

#### 3.1. Variation of applied, recovery and effective stress with applied strain

Previously, it was mentioned that the partitioning of the applied stress into recovery and effective stress components was made in order to facilitate detailed investigations of the deformation behaviour. Such partitioning will then differentiate the effect of processes which store elastic energy during deformation and hence sustain some of the applied stress, from the remainder of the stress which is responsible

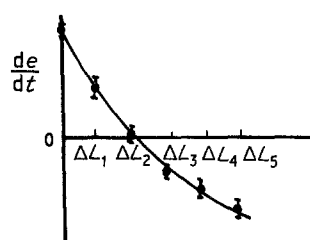


Figure 5 A plot of load reduction ( $\Delta L$ ) against extension rate ( $de/dt$ ).

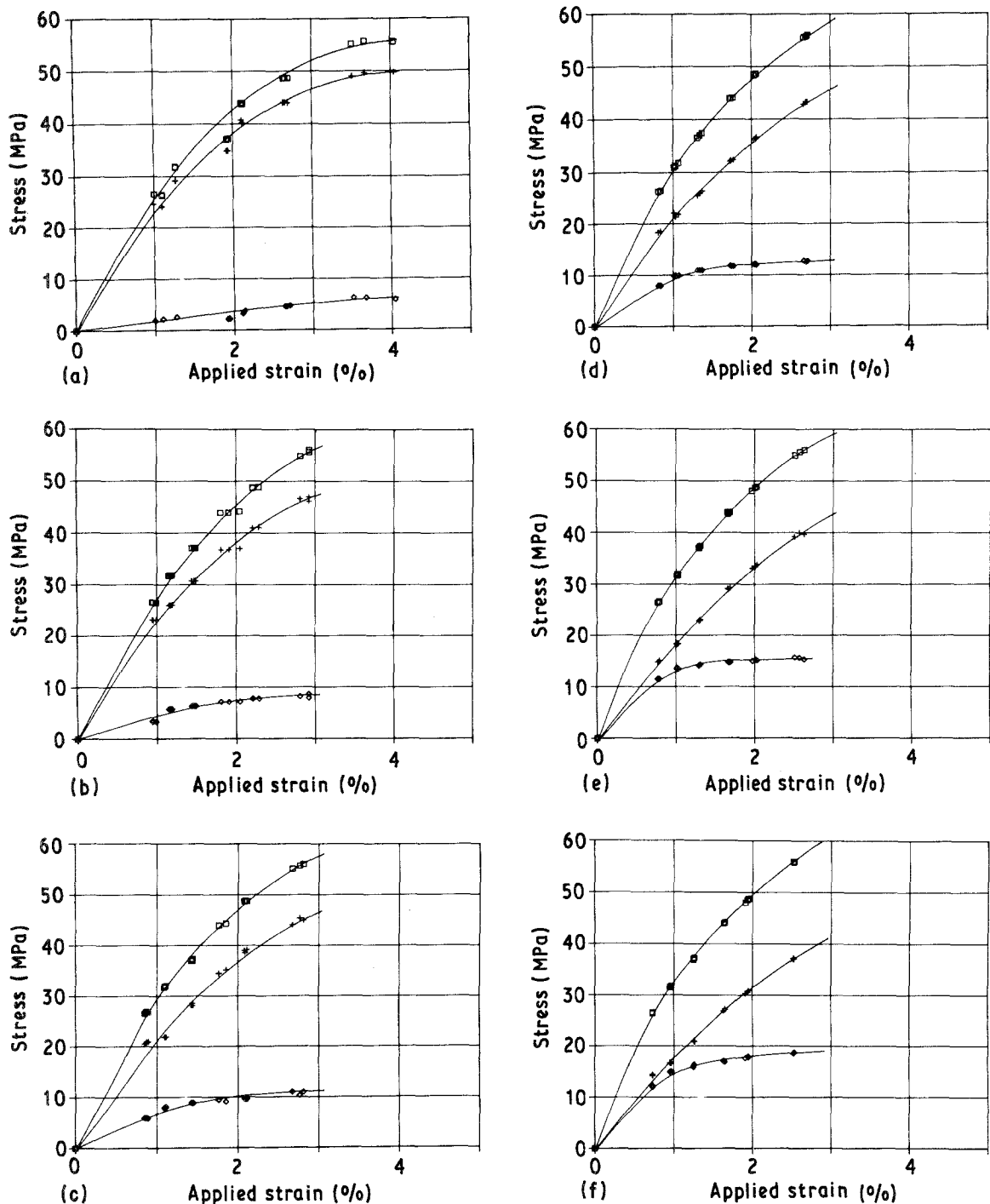


Figure 6 Variation of (□) applied, (+) recovery and (◇) effective stresses with applied strain. Value of CHS (cm min<sup>-1</sup>): (a) 0.05, (b) 0.10, (c) 0.20, (d) 0.50, (e) 1.00, (f) 2.00.

for the viscous processes that are amenable to a conventional treatment of thermally activated flow.

Fig. 6 shows the plot of the three stresses (applied, recovery and effective) against applied strain for cross-head speeds (CHS) ranging from 0.05 to 2.00 cm min<sup>-1</sup>. An obvious result is that as the crosshead speed increases, the maximum value of the effective stress increases while the recovery stress decreases. The magnitude of the effective stress, at each crosshead speed, is relatively smaller than the rest and appears to approach a limiting value at larger applied strains. This limiting stress value ranges from about 5 MPa at 0.05 cm min<sup>-1</sup> to 20 MPa at 2.00 cm min<sup>-1</sup>.

It is interesting to note that as the crosshead speed increases, the recovery stress deviates further from the applied stress. It appears that the general increase in

applied stress, at fixed applied strain, with CHS is probably due to the increase in effective stress and not the recovery stress, an important discovery which has not been noted before for PVC.

### 3.2. Variation of recovery stress with applied stress

Earlier work carried out by Fotheringham and Cherry [1] who did their experiments in compression and under a stress transient dip test, revealed that an upper limit, defined by  $\sigma_{re} = 0.78 \sigma_{ap}$ , exists for high-density polyethylene. An attempt is made here to see whether such a relationship is also true for PVC tested under the present conditions.

Fig. 7 shows the plot of recovery stress against applied stress. As the crosshead speed decreases, it can

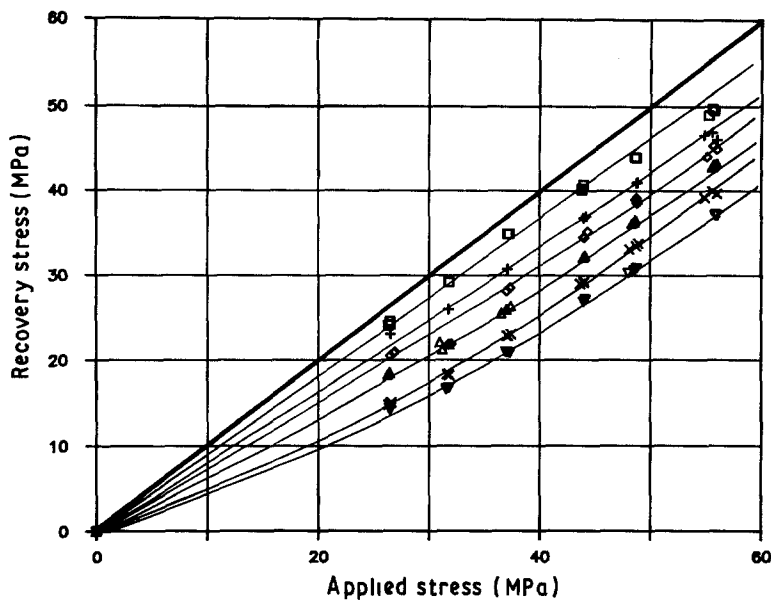


Figure 7 Variation of recovery stress with applied stress. Values of CHS ( $\text{cm min}^{-1}$ ): ( $\square$ ) 0.05, (+) 0.10, ( $\diamond$ ) 0.20, ( $\Delta$ ) 0.50, (x) 1.00, ( $\nabla$ ) 2.00.

be seen that the recovery stress approaches that of the applied stress; the upper stress limit then appears to be defined by  $\sigma_{re} = \sigma_{ap}$  (bold line in Fig. 7). This deduction is not presumptuous, since from Equation 1 as  $\sigma_{er} \rightarrow 0$  at low crosshead speeds, the maximum value  $\sigma_{re}$  could have is  $\sigma_{ap}$ . At the present moment it cannot be proven conclusively whether this different relationship between  $\sigma_{re}$  and  $\sigma_{ap}$  is due to the different testing conditions and/or to the different morphological structure of the specimens (since high-density polyethylene is semicrystalline and PVC is almost amorphous). If it is due to the latter, then important indications can be derived to suggest possible effects of the semicrystalline state on the effective stress portion. However, it needs to be emphasized that the testing conditions as illustrated in Fig. 4 are such that the initial deformation is applied using a constant strain rate, and the internal stress measurements are determined by recording the extension rate after a series of constant-load interruptions. These conditions are different from the stress transient dip tests where the internal stresses are determined by some stress relaxation technique. Here the applied strain is held con-

stant and the stress monitored as a function of time [1].

### 3.3. Variation of effective stress with applied strain

Fig. 6 shows that the effective stress approaches a limiting value for each CHS and that the yield point is difficult to define when one looks closely at the applied stress against applied strain. In order to study this further, a plot of effective stress against applied strain (with expanded scale for the effective stress) is made in Fig. 8. From this figure, one interesting feature can be seen, that is, one can define the extrapolated yield point (EYP) [1] quite clearly by drawing tangents as shown. (This further adds weight to the usefulness of partitioning the applied stress for detailed deformation studies.) With the exception of the low strain rate of  $0.05 \text{ cm min}^{-1}$ , where EYP is not so obvious, the general trend seems to be that the EYP increases with increasing CHS.

The association of effective stress with yield behaviour was also previously found to be true for high-density polyethylene [1]. If the effective stress portion

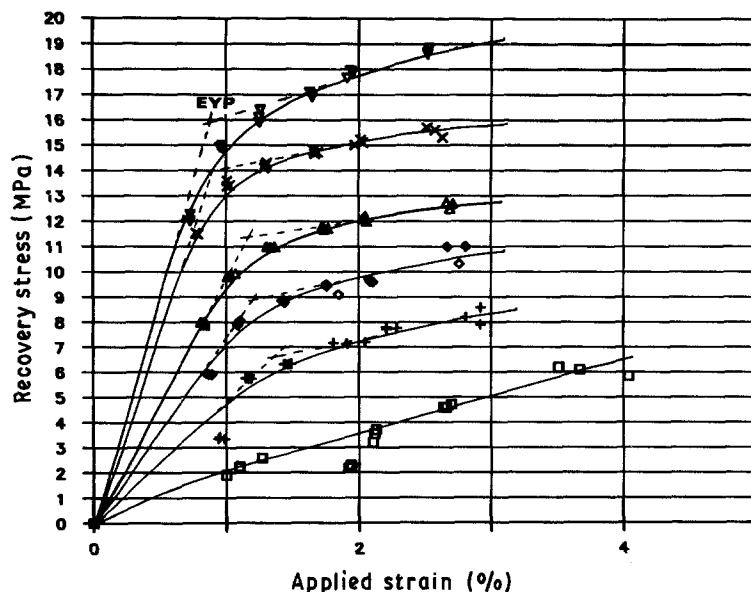


Figure 8 Variation of effective stress with applied strain. Values of CHS ( $\text{cm min}^{-1}$ ): ( $\square$ ) 0.05, (+) 0.10, ( $\diamond$ ) 0.20, ( $\Delta$ ) 0.50, (x) 1.00, ( $\nabla$ ) 2.00.

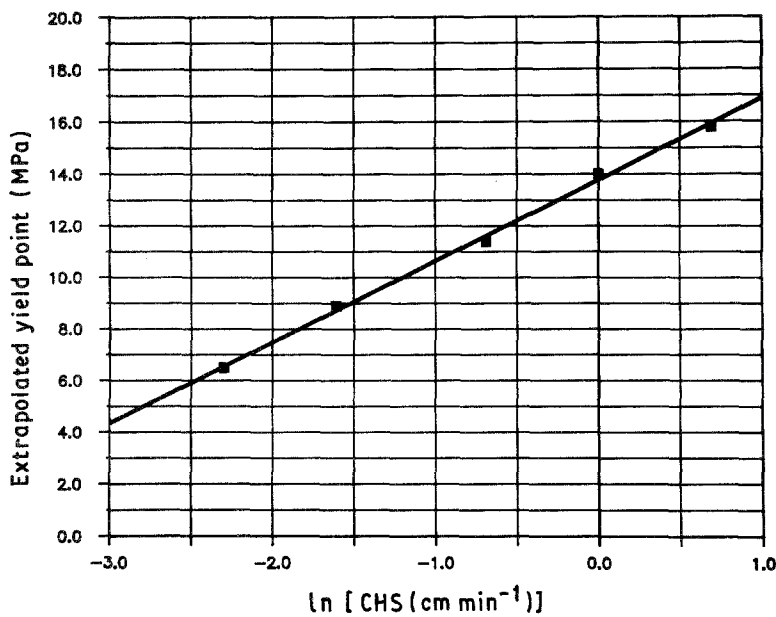


Figure 9 A plot of extrapolated yield point (EYP) against the natural logarithm of crosshead speed (CHS).

can be represented by a rate-activated dashpot [6], then the viscous process can be amenable to a conventional treatment of thermally activated flow after Eyring [5]. Fig. 9 shows a plot of EYP against the natural logarithm of CHS. A straight line defined by

$$\text{EYP} = 13.71 + 3.10 \ln(\text{CHS}) \quad (11)$$

is obvious. The slope of the line has a gradient of 3.10. The gradient is a function of the activation volume,  $V$ . If Eyring's equation is simplified to

$$\sigma = A + \frac{2kT}{V} \ln(\text{CHS}) \quad (12)$$

where  $A$  is a constant,  $k$  is Boltzmann's constant and  $T$  is the absolute temperature, one can readily calculate the activation volume  $V$  which is  $2.64 \text{ nm}^3$ . Although it is not the intention of the paper to discuss the significance of this value, it is noted that this value is of the same magnitude as that measured by Haward and Thackray [22].

### 3.4. Variation of the ratio of effective stress to recovery stress with applied strain

In order to determine whether the energy-dissipation

(viscous flow) portion or the energy-storage portion of the material plays a more important role as the deformation proceeds, one needs to look at the variation of the ratio of effective stress to recovery stress with applied strain. This is shown in Fig. 10. Here it can be seen that this ratio increases to a maximum and then falls off gradually at higher strains. It is interesting to note that there exists a peak ratio for each crosshead speed (with the exception of  $\text{CHS} = 0.05 \text{ cm min}^{-1}$ , where the peak is less obvious). This peak ratio increases with CHS (dotted line) and occurs between 0.85 and 1.32% applied strain.

The shapes of these curves suggest that the role of the effective stress portion, which is related to the viscous flow of the rate-activated (energy-dissipation) process, appears to be more dominant during the early stages of deformation; while the recovery stress portion, which is related to the energy-storage part of the material, appears to take over during the latter stages of deformation at fixed CHS.

The peak ratio was also seen to increase with CHS. This is an important result as it could suggest that at high rates of straining (for example during impact) where the strain to failure is, say, below 0.85%, the

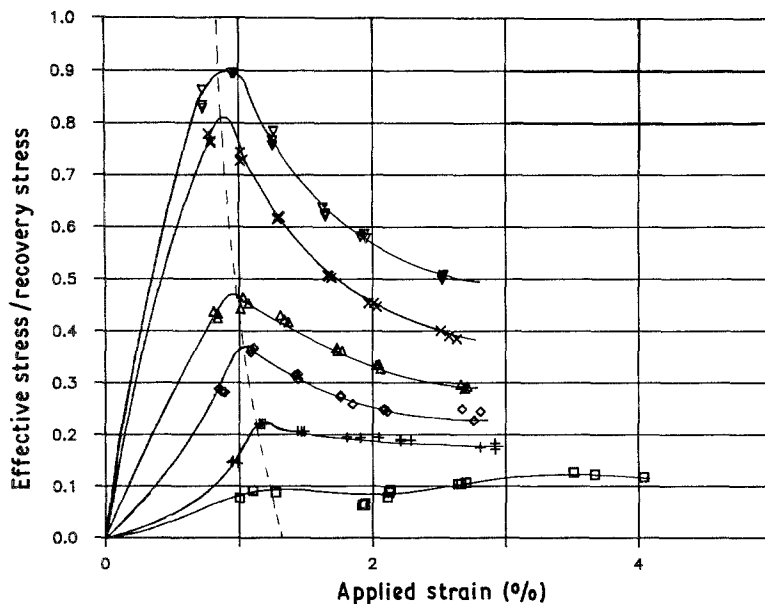


Figure 10 Variation of the ratio of effective stress to recovery stress with applied strain. Values of CHS ( $\text{cm min}^{-1}$ ): (□) 0.05, (+) 0.10, (◇) 0.20, (△) 0.50, (×) 1.00, (▽) 2.00.

effective stress portion is dominant, while at low rates of straining (for example during long-term creep testing) the recovery stress portion is dominant. However, at this early stage it is not conclusive as yet to confirm this trend of behaviour. This will be a subject of future research. More sensitive equipment involving fast-responding and low-friction servohydraulics is currently under development. This will be used to confirm that the results obtained are not due to the sensitivity of the machine but rather the actual material property. Future work will also involve the application of this modified strain transient dip test to creep loading.

#### 4. Conclusion

A simple technique based on a modified strain transient dip test involving rapid unloading and extrapolating to zero extension rate has been shown to be useful in determining the internal stress components of PVC under uniaxial tension.

From the variations of applied, recovery and effective stresses with applied strain it was found that

(a) the effective stress component approaches a limiting value as the applied stress increases. These limiting stress values range from a value of 5 MPa at 0.05 cm min<sup>-1</sup> to 20 MPa at 2.00 cm min<sup>-1</sup>, indicating that they are a function of the strain rate during the initial load application;

(b) an extrapolated yield point could be defined only for the variation of effective stress with applied strain; this yield point increases with crosshead speed and is amenable to analysis using the rate-activated process (following Eyring's equation) with an activation volume of 2.64 nm<sup>3</sup>, and

(c) the general increase in applied stress (at fixed applied strains) with crosshead speed is due to the increase in effective stress, and not to the recovery stress which appears to be a dominant component at low crosshead speeds.

From the variations of applied stress and recovery stress, an upper limit could be defined by  $\sigma_{re} = \sigma_{ap}$  for PVC, an expression different to that reported earlier [1] for high-density polyethylene.

By plotting the ratio of effective stress to recovery stress against applied strain it was determined that a maximum peak ratio exists at each crosshead speed. This peak ratio increases with crosshead speed, and

could indicate that it was the energy-dissipation part of the material that played a dominant role in the early stages of the deformation, while the energy-storage part dominated the latter stages.

#### Acknowledgements

The authors gratefully acknowledge a research grant (RP22/83) from the National University of Singapore, and Mr Na Wee Kwong for his assistance in data collection and preliminary experimental set-up.

#### References

1. D. G. FOTHERINGHAM and B. W. CHERRY, *J. Mater. Sci.* **13** (1978) 951.
2. D. M. SHINOZAKI and C. M. SARGENT, *Mater. Sci. Engng.* **35** (1978) 213.
3. A. ORLOVA, M. PAHUTOVA and J. CADEK, *Phil. Mag.* **25** (1972) 865.
4. A. A. SOLOMON, C. N. AHLQUIST and W. D. NIX, *Scripta Metall.* **4** (1970) 231.
5. H. EYRING, *J. Chem. Phys.* **4** (1936) 283.
6. S. H. TEOH, PhD thesis, Monash University, Australia (1982).
7. J. J. JONAS, *Acta Metall.* **17** (1969) 397.
8. J. C. M. LI, *Can. J. Phys.* **45** (1967) 493.
9. C. N. AHLQUIST and W. D. NIX, *Scripta Metall.* **3** (1969) 679.
10. B. BERGMAN, *Scand. J. Metall.* **4** (1975) 109.
11. N. PAHUTOVA, J. CADEK and P. RYS, *Mater. Sci. Engng.* **34** (1979) 169.
12. A. ORLOVA, *Scripta Metall.* **13** (1979) 763.
13. C. G'SELL and J. J. JONAS, *J. Mater. Sci.* **16** (1981) 1956.
14. J. KUBAT and M. RIGDAHL, *Int. J. Polym. Mater.* **3** (1975) 287.
15. P. W. DAVIES, G. NELMES, K. R. WILLIAMS and B. WILSHIRE, *Met. Sci. J.* **7** (1973) 87.
16. D. SIDEY, *Met. Trans.* **7A** (1976) 1785.
17. J. GITTUS, "Creep, Viscoelasticity and Creep Fracture of Solids" (Applied Science, London, 1975) p. 50.
18. L. J. CUDDY and J. C. RALEY, *Acta Metall.* **21** (1973) 427.
19. W. J. EVANS and G. F. HARRISON, *J. Mater. Sci.* **10** (1975) 307.
20. A. S. KRAUSZ and H. EYRING, "Deformation Kinetics," (Wiley, New York, 1975) p. 260.
21. R. F. STAATS-WESTOVER and S. MATSUOKA, in Proceedings of SPE 40th Annual Technical Conference, San Francisco, May 1982 p. 25.
22. R. N. HAWARD and G. THACKRAY, *Proc. R. Soc. A302* (1968) 453.

Received 5 May  
and accepted 4 September 1986